Publications of the Astronomical Society of Australia (2024), **41**, e104, 7 pages
doi:10.1017/pasa.2024.89

CAMBRIDGE UNIVERSITY PRESS

Research Article

On the collisional sensitivity of polarised Mg II solar lines

M. Derouich and S. Qutub

Astronomy and Space Science Department, Faculty of Science, King Abdulaziz University, P.O. Box 80203, Jeddah 21589, Saudi Arabia

Abstract

Neutral and singly ionised states of the magnesium (Mg) are the origin of several spectral lines that are useful for solar diagnostic purposes. An important element in modelling such solar lines is collisional data of the Mg with different perturbers abundant in the Sun, specially with neutral hydrogen. This work aims at providing complete depolarisation and polarisation and population transfer data for Mg II due to collisions with hydrogen atoms. For this purpose, a general formalism is employed to calculate the needed rates of MgII due to collisions with hydrogen atoms. The resulting collisional rates are then employed to investigate the impact of collisions on the polarisation of 25 Mg II lines relevant to solar applications by solving the governing statistical equilibrium equations within multi-level and multi-term atomic models. We find that the polarisation of some Mg II lines starts to be sensitive to collisions for hydrogen density $n_H \gtrsim 10^{14}$ cm^{-3}.

Keywords: Collisions; atomic processes; polarisation; sun: chromosphere; line: formation

(Received 14 July 2024; revised 21 September 2024; accepted 25 September 2024)

1. Introduction

Magnesium is abundant in the solar atmosphere, and its neutral and singly ionized states give rise to numerous spectral lines with significant diagnostic potential in the photosphere, chromosphere, and the transition region. NASA's Interface Region Imaging Spectrograph (IRIS) spacecraft provided an important opportunity to observe intensity spectra of several lines, including the Mg II lines. Various works have presented forward modelling of the intensity of Mg II lines (e.g. Leenaarts et al. 2013).

Polarisation spectra of Mg II h-k lines have been observed through the Ultra-Violet Spectro-Polarimeter on board the Solar Maximum Mission (Calvert et al. 1979, Bohlin et al. 1980, Woodgate et al. 1980). These measurements have been analysed by Henze & Stenflo (1987). Furthermore, several theoretical studies have improved our comprehension of the physical processes that cause the polarisation of the Mg II h-k lines, highlighting their magnetic sensitivity (e.g. Auer et al. 1980, Henze & Stenflo 1987, Belluzzi & Trujillo Bueno 2012; Alsina Ballester et al. 2016; del Pino Alemán et al. 2016, 2020). In addition, UV spectropolarimeter called Chromospheric LAyer SpectroPolarimeter (CLASP2) was launched on 2019 to observe polarized light emitted by Mg II ions around the wavelength of 280 nm for investigating the magnetic properties of the transition region and the upper chromosphere.

Our aim is to contribute to the efforts concentrated on observing and interpreting Mg II lines by elucidating the possible collisional depolarising role during their formation. In fact, collisions with hydrogen might be important for modelling chromospheric Mg II lines and their depolarising effect has not been elucidated in details previously.

We model the Mg II by a multi-level and then by a more realistic multi-term atomic model (see Landi Degl'Innocenti & Landolfi 2004). We provide all needed collisional rates due to the Mg II+H collisions. We include these rates in the statistical equilibrium equations (SEE) for multi-level and multi-term atomic models, which are then solved to determine how collisions impact the polarisation of the Mg II lines.

2. Collisional effects in multi-level case

2.1 SEE collisional contribution

We adopt the LS coupling scheme, where the level is usually denoted by $nl\,^{2S+1}L_J$, where n is the principal quantum number, l is the orbital angular momentum quantum number, S is the total spin, L is the total orbital angular momentum, and J is the total angular momentum defined as $J = L + S$ (e.g. Martin & Wiese 2002). For simplicity, we will also use the notations $nl\,^{2S+1}L_J = nl\,LS\,J = \alpha J$, where α represents the set of quantum numbers $(n\,l\,LS)$. In the context of the polarisation studies, the representation of Mg II states using the atomic density matrix formalism based on irreducible tensorial operators is demonstrated to be the most appropriate (e.g. Sahal-Bréchot 1977; Landi Degl'Innocenti & Landolfi 2004). In this basis, the contribution of depolarising isotropic collisions to the SEE is given by (e.g. Sahal-Bréchot et al. 2007):

$$\left(\frac{d\,\rho^k_q(\alpha\,J)}{dt}\right)_{\rm coll} = -\,D^k(\alpha\,J,T)\,\rho^k_q(\alpha\,J) - \rho^k_q(\alpha\,J)\sum_{J'\neq J}\sqrt{\frac{2J'+1}{2J+1}}D^0(\alpha\,J\to\alpha\,J',T) + \sum_{J'\neq J}D^k(\alpha\,J'\to\alpha\,J,T)\,\rho^k_q(\alpha\,J')\,, \quad (1)$$

Corresponding author: M. Derouich; Emails: aldarwish@kau.edu.sa & derouichmoncef@gmail.com

Cite this article: Derouich M and Qutub S. (2024) On the collisional sensitivity of polarised Mg II solar lines. *Publications of the Astronomical Society of Australia* **41**, e104, 1–7. https://doi.org/10.1017/pasa.2024.89

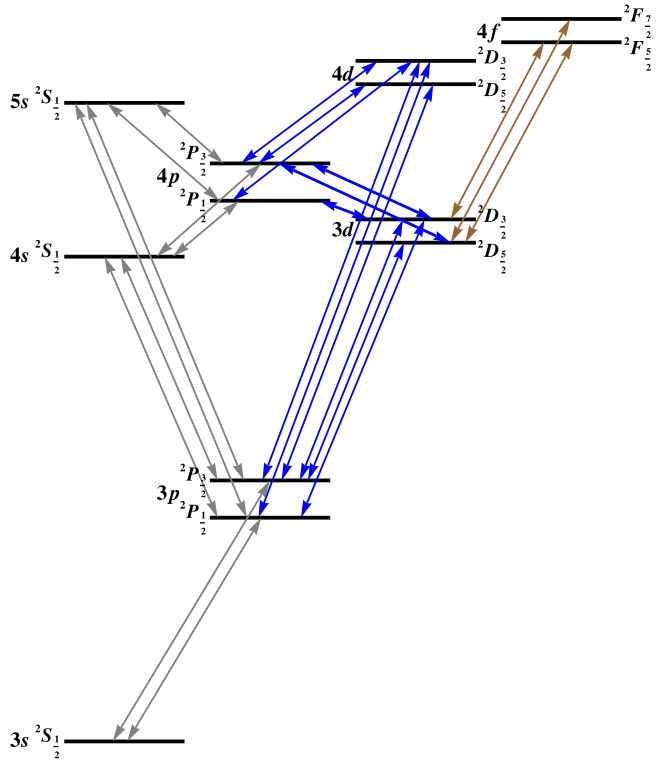

Figure 1. Energy diagram of the atomic model of Mg II adopted for this work. Note that $p-d$ transitions taken into account are represented in blue, $s-p$ transitions are represented in grey, and $f-d$ transitions are represented in brown colour.

where k, $0 \leq k \leq k_{\rm max}$, is the tensorial order with $k_{\rm max}$=$2J$ for J=J' and $k_{\rm max}$=$min\{2J, 2J'\}$ for $J \neq J'$. $D^k(\alpha\, J, T)$ and $D^k(\alpha\, J \rightarrow \alpha\, J', T)$ are the depolarisation and the polarisation transfer rates, respectively. Note that $D^0(\alpha\, J \rightarrow \alpha\, J', T)$ is the population transfer rate between the levels $(\alpha\, J)$ and $(\alpha\, J')$. These rates should be calculated independently to enter the SEE. To model the Mg II ions, we consider a comprehensive atomic model containing large number of lines ranging from the ultraviolet to the infrared as shown in Figure 1 (see also Fig. 1 of Leenaarts et al. 2013).

2.2 Collisional rates for P-, D-, and F-states

The atomic model adopted in this paper contains s-, p-, d-, and f-states (see Figure 1). Note that s-states of the present model are not linearly polarisable and, therefore, are not affected by collisions with hydrogen atoms. The rates $D^k(\alpha\, J, T)$ and $D^k(\alpha\, J' \rightarrow \alpha\, J, T)$ for the levels of the $3p\ ^2P$ term have been previously calculated using the hybrid method developed by Derouich (2020). In order to obtain the rates associated to the other terms of Figure 1: $4p\ ^2P$, $3d\ ^2D$, $4d\ ^2D$, and $4f\ ^2F$, one can either employ a direct calculation by running the numerical code of collisions for each level as explained in the formalism presented by Derouich et al. (2004) or use the genetic programming (GP) functions presented in Derouich (2017) for p-states, Derouich et al. (2017) for d-states and Derouich (2018) for f-states.

Whether running the numerical code of collisions or using the GP functions, it is necessary to determine the Unsöld energy E_P for each ionic state. This energy must then be used as input for either the numerical code or the GP functions. In addition to E_P,

Table 1. Mg II atomic and collisional parameters for the multi-level case

Term	E_p (a.u.)	C_6 (a.u.)	n^*	$<r^2>$ (a.u.)
$4p\ ^2P$	−0.42665	310.02	3.286	66.12
$3d\ ^2D$	−0.4636	133.56	2.990	30.96
$4d\ ^2D$	−0.4496	536.99	3.962	120.71
$4f\ ^2F$	−0.4431	404.82	3.997	89.69

Note that the collisional rates as they are presented in this section depend on the precision of the calculation of E_p, which is related to the precision of C_6 obtained from the Kurucz methodology and $<r^2>$ resulting from the hydrogenic approximation. To examine the dependence of the depolarisation rates.

the effective quantum number n^* is also needed as input parameter. If the energy of the state $|a\rangle$ of the valence electron is E_a and the ionisation energy of the ion is E_∞, the effective quantum number n^* is given by (see, e.g., Derouich 2004):

$$n^* = 2 \times [2(E_\infty - E_a)]^{-1/2} \tag{2}$$

where the energies are in atomic units. Values of n^* are provided in Table 1 for all the cases where n^* is required to determine the collisional rates. Appropriate value of E_p can then be calculated from the Unsöld formula (see, e.g., Barklem & O'Mara 1998):

$$E_p = -\frac{2 <r^2>}{C_6}, \tag{3}$$

in atomic units, where C_6 is the van der Waals coefficient (see Table 1), and $<r^2>$ is the average of the squared distance between the electron of valence and the nucleus of the perturbed ion (see Table 1). By adopting the hydrogenic approximation, one has for singly ionized atoms (see, e.g., Barklem 1998):

$$<r^2> = \frac{n^{*2}}{8}[5n^{*2} + 1 - 3l(l+1)]. \tag{4}$$

The van der Waals coefficients are available on Kurucz's website (Kurucz 2013; kurucz.harvard.edu), namely the file "gammasum1201z.gam" which contains comprehensive information on the Mg II lines and relevant atomic parameters. For the 3 $d\ ^2D$ state,

$$C_6^{\rm Kurucz}(\text{ Mg II}, 3d\ ^2D) = 1.93 \times 10^{-32}\ \text{cm}^6\ \text{s}^{-1} \tag{5}$$

Note that the definition of C_6 included in Equation 3 giving E_p differs by a factor of h (h is the Planck constant) from $C_6^{\rm Kurucz}$, in addition to the difference in units since C_6 of Equation 3 is in a.u. while $C_6^{\rm Kurucz}$ is in cm^6 s^{-1}. In fact,

$$\begin{aligned} C_6(\text{ Mg II}, 3d\ ^2D) &= 6.92 \times 10^{33}\ C_6^{\rm Kurucz}(\text{ Mg II}, 3d\ ^2D) \\ &= 133.56\ \text{ a.u.}, \end{aligned} \tag{6}$$

implying that:

$$E_p = -0.464\ \text{a.u.} \tag{7}$$

Similar calculation allows us to obtain all E_p values needed for the computation of depolarisation and polarisation and population transfer rates (see Table 1).

Our depolarisation and polarisation transfer rates are written in the form $D^k = a^k \times 10^{-9}\ n_H \left(\frac{T}{5000}\right)^{\lambda^k}$. Note that $a^k \times 10^{-9} = D^k/n_H$ at $T = 5000$ K and λ^k is the so-called velocity exponent (e.g. Derouich et al. 2004). Values of a^k and λ^k with even k-order, which are relevant for linear polarisation treatment within the multi-level

https://doi.org/10.1017/pasa.2024.89 Published online by Cambridge University Press

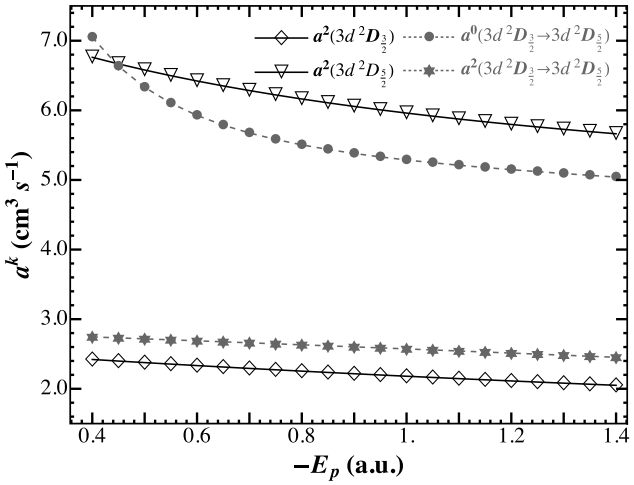

Figure 2. Variation of the collisional rates with E_p.

model, are provided in Table 2 (see Appendix 1). In particular, we provide only $D^k(\alpha\, J\rightarrow\alpha\, J')$ since $D^k(\alpha\, J'\rightarrow\alpha\, J)$ are calculated by applying the detailed balance relation:

$$D^k(\alpha\, J'\rightarrow\alpha\, J)=\frac{2J+1}{2J'+1}\exp\left(\frac{E_{J'}-E_J}{k_BT}\right)D^k(\alpha\, J\rightarrow\alpha\, J') \qquad (8)$$

with k_B is the Boltzmann constant and E_J is the energy of the J-level.

$D^2(3d\,^2D_{\frac{3}{2}})$ and $D^2(3d\,^2D_{\frac{5}{2}})$ and transfer rates $D^2(3d\,^2D_{\frac{3}{2}}\rightarrow 3d\,^2D_{\frac{5}{2}})$ and $D^0(3d\,^2D_{\frac{3}{2}}\rightarrow 3d\,^2D_{\frac{5}{2}})$ to E_p, we study the sensitivity of the a^k coefficients to the E_p variation. As it can be seen in Figure 2, the a^k are sufficiently stable with respect to sensible variation of E_p. The range of the calculation presented in Figure 2 is chosen to contain possible values of E_p, based on different models, such as the one adopted by O'Mara & Barklem (1998) for the $3d\,^2D$ state of the Ca II, where E_p was found to be between -0.918 and -1.236 a.u.

2.3 Resolution of the SEE in the multi-level case

We consider a slab of Mg II ions positioned at the solar atmosphere, and we assume a zero-magnetic field case. To generate a polarized light, the slab of Mg II ions is assumed to be illuminated from below by anisotropic solar radiation. The components of the incoming radiation field are typically represented by J^k_q, where k is the tensorial order and q signifies the coherences in the tensorial basis ($-k\leq q\leq k$). The atmospheric light is considered to be uniform and exhibits cylindrical symmetry about the local solar vertical at the scattering center (the Mg II ion) which implies that, for a given frequency ν, only $J^0_0(\nu)$ and $J^2_0(\nu)$ are non-zero. The components $J^0_0(\nu)$ and $J^2_0(\nu)$ are given by the number of photons per mode $\bar{n}(\nu)=J^0_0\,(c^2/2h\jmath^0_0(\nu)^3)$ and the value of the anisotropy factor $w(\nu)=\sqrt{2}\,(J^2_0/J^0_0)$ (see e.g. Derouich et al. 2007). Calculations of the non-zero components of the incident radiation field, $J^0_0(\nu)$ and $J^2_0(\nu)$, for each line are based on Cox (2000) (see also Allen & Cox 1999, Thuillier et al. 2004).

The anisotropic incident radiation field induces population imbalances and coherences between the Zeeman sublevels of a given (αJ)-level of the Mg II ions. These population imbalances and coherences are referred to as atomic polarisation. Under these conditions, owing to the cylindrical symmetry of the problem, only linear polarisation is produced by scattering, and only the density matrix elements with $q=0$ and k even are non-zero. The statistical equilibrium equations (SEE) include 26 unknowns, corresponding to the density matrix elements ρ^k_0.

The Einstein coefficients required for the radiative rates entering the SEE are extracted from NIST database. In addition to the expressions of the radiative rates, which are taken from Landi Degl'Innocenti & Landolfi (2004), the numerical code incorporates the collisional rates, given in Table 2, as input to compute the values of the atomic density matrix elements. These values are affected by the gain terms called collisional polarisation transfer rates and denoted by $D^k(\alpha\, J'\rightarrow\alpha\, J)$, and by the loss (collisional relaxation) terms $D^k(\alpha\, J)+\sqrt{\frac{2J'+1}{2J+1}}D^0(\alpha\, J\rightarrow\alpha\, J',T)$ (see Equation (1)).

Our focus is on the effects of elastic collisions with neutral hydrogen to complement existing studies that omit these collisions. While a more comprehensive analysis of Mg II line polarisation would include processes such as collisions with electrons and polarized radiative transfer in a magnetized atmosphere; these are beyond the scope of this paper.

Given that collisional rates are proportional to the hydrogen density n_H (according to the impact approximation), analyzing how polarisation depends on collisional rates is equivalent to examining its dependence on n_H. In theory, even if the core of a line is formed at higher chromospheric layers, its wings can be formed in deeper layers of the chromosphere. Given that the density of hydrogen atoms n_H is larger in deep chromospheric layers and that the considered lines cover spectral window from the ultraviolet to the infrared, one should perform a scan over large range of n_H values. We solve the SEE to calculate the non-zero ρ^k_0 elements by adopting the multi-level atomic model presented in the Figure 1 for a wide range of hydrogen density values n_H going from 10^{12} cm^{-3} to 10^{19} cm^{-3} while adopting a solar temperature $T=5000$ K. We point out the range of n_H where the effect of collisions is important.

In Figure 3, we shows the ratio $\frac{\rho^{k=2}_0(n_H)}{\rho^{k=2}_0(n_H=0)}$ giving the variation of the alignment as a function of n_H. It can be seen that collisions start influencing the alignment of the $4p\,^2P_{3/2}$ level for $n_H\sim 10^{14}$ cm^{-3}. Consequently, the 6 lines directly connected to this level (see Figure 1) should be affected by collisions for $n_H\gtrsim 10^{14}$ cm^{-3}. Lines with upper and/or lower levels different from the $4p\,^2P_{3/2}$ could be also indirectly slightly affected for $n_H\gtrsim 10^{14}$ cm^{-3} due to the coupling between the different levels through the SEE. All the levels other than $4p\,^2P_{3/2}$ start to be depolarized for $n_H\gtrsim 10^{15}$ cm^{-3}.

3. Multi-term case

In this section, we will allow for coherences between different (αJ) and $(\alpha J')$-levels grouped within the same term $n\,l\,^{2S+1}L$. The density matrix elements associated to these coherences are denoted by $\rho^k_q(\alpha\, JJ')$. This is the so-called mutli-term case (see Section 7.5 of Landi Degl'Innocenti & Landolfi 2004). Indeed, a more realistic diagnostic of the polarisation of the lines of Mg II should be performed in the framework of the multi-term atomic model due to the tiny energy separation between the levels of the d- terms and similarly between those of the f-terms. We consider the atomic model of Mg II shown in Figure 1, with eight terms: $3\,s\,^2S$, $3\,p\,^2P$, $4\,s\,^2S$, $3\,d\,^2D$, $4\,p\,^2P$, $5\,s\,^2S$, $3\,d\,^2D$ and $4\,f\,^2F$; we take into account coherences between different J-levels within these terms. In fact,

https://doi.org/10.1017/pasa.2024.89 Published online by Cambridge University Press

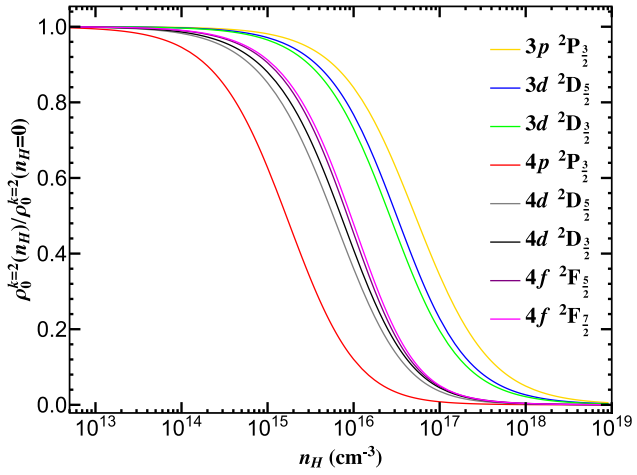

Figure 3. Variation of the ratio $\frac{\rho_0^2(n_H)}{\rho_0^2(n_H=0)}$ as a function of n_H for the Mg II levels within the framework of the multi-level model.

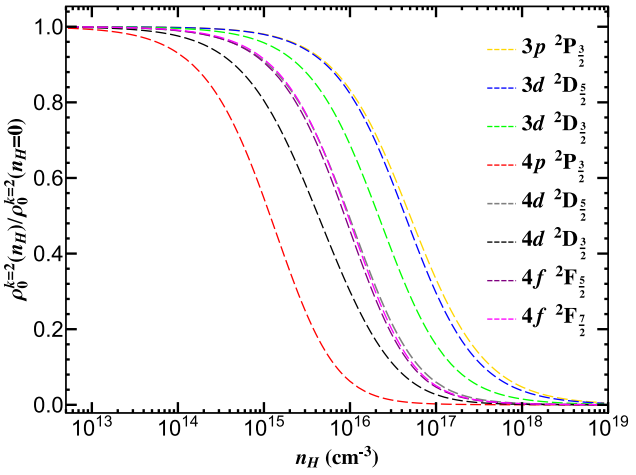

Figure 4. Same as Figure 3 but for the multi-term model.

In the spherical statistical tensors representation, the contribution of the isotropic collisions to the SEE in the multi-term case is:

$$\left(\frac{d\,\rho_q^k(\alpha\,JJ')}{dt}\right)_{\rm coll} = -\left[\sum_{(J''J''')\neq(JJ')}\sqrt{\frac{J''+J'''+1}{J+J'+1}}\,D^0(\alpha\,JJ'\rightarrow\alpha\,J''J''') + D^k(\alpha\,JJ')\right]\times\rho_q^k(\alpha\,JJ') + \sum_{(J''J''')\neq(JJ')} D^k(\alpha\,J''J'''\rightarrow\alpha\,JJ')\times\rho_q^k(\alpha\,J''J''') \quad (9)$$

Note that J, J', J'', and J''' represent possible values of the total angular momentum within the same term $n\,l\,^{2S+1}L$.

The radiative contributions are taken from multi-term atomic model as described by Landi Degl'Innocenti & Landolfi (2004). In order to calculate $\rho_q^k(\alpha\,JJ')$, we need the depolarisation rates $D^k(\alpha\,JJ')$ and the polarisation/population transfer rates $D^k(\alpha\,JJ'\rightarrow\alpha\,J''J''')$ with $(JJ')\neq(J''J''')$ due to collisions of H atoms in their ground state $^2S_{1/2}$ with Mg II presented by the eight-term atomic model adopted in this work. Direct calculation of the $D^k(\alpha\,JJ')$ and $D^k(\alpha\,JJ'\rightarrow\alpha\,J''J''')$ rates is a complicated task since one should take into account the coherences between J-levels when calculating the interaction potential and solving the Schrödinger equation. At the best of our knowledge, this direct calculation have not been performed neither theoretically nor experimentally. To address this problem, one can adopt an indirect and more practical method, based on the frozen spin S approximation. Using this approach, one can show that:

$$D^k(\alpha\,JJ'\rightarrow\alpha\,J''J''') = \sqrt{(2J+1)(2J'+1)(2J''+1)(2J'''+1)}\times\sum_{k_L}(2k_L+1)\,D^{k_L}(n\,l\,L)\times\sum_{k_S}(2k_S+1)\begin{Bmatrix}L & S & J\\ L & S & J'\\ k_L & k_S & k\end{Bmatrix}\begin{Bmatrix}L & S & J''\\ L & S & J'''\\ k_L & k_S & k\end{Bmatrix} \quad (10)$$

Equation (10) is obtained through a methodology which is formally similar to that firstly proposed by Nienhuis (1976) and Omont (1977) (see also Derouich & Barklem 2007 and Sahal-Bréchot et al. 2007). We note that diagonal rates $J=J'$ and $J''=J'''$ are similar to the transfer rates used for the case of multi-level atomic models. However, calculation of the off-diagonal rates (i.e. $J\neq J'$ and/or $J''\neq J'''$) requires the evaluation of the tensorial rates $D^{k_L}(n\,l\,L)$ (see Equation (10)). Since the Mg II is a simple ion modelled as a single valence electron outside a spherical ionic core, one has $D^{k_L}(n\,l\,L)=D^{k_l}(n\,l)$ where $L=l$ is the angular momentum of the optical electron (see Derouich et al. 2005 and Sahal-Bréchot et al. 2007).

The main step to obtain $D^{k_l}(n\,l)$, needed in Equation (10), is the calculation of the scattering matrix. We ran our numerical code to solve the coupled differential equations and obtain the scattering matrix elements in the basis $|lm_l\rangle$ for a given velocity and impact parameter b (where m_l is the projection of l along the quantization axis; see Derouich et al. 2003a,b; Derouich et al. 2004). We then obtained the $D^{k_l}(n\,l)$ rates through an integration over the impact parameter b and the Maxwell distribution of velocities (see Equations 7, 9, 12, and 20 of Derouich et al. 2003a).

All the non-zero depolarization and polarization transfer rates are written in the form

$$D^k = a^k\times10^{-9}\,n_H\left(\frac{T}{5000}\right)^{\lambda^k} \quad (11)$$

and are tabulated in the Tables 3, 4, 5, and 6. Note that, in particular, $D^k(\alpha\,JJ\rightarrow\alpha\,J'J')=D^k(\alpha\,J\rightarrow\alpha\,J')$ are related to $D^k(\alpha\,J'J'\rightarrow\alpha\,JJ)$ through the usual detailed balance relation (see Equation (8)). We compute all the non-zero density matrix elements with even k-order which are 44 in the case of our multi-term atomic model of Figure 1. The results obtained for some diagonal elements $\rho_q^{k=2}(\alpha JJ)$ are presented in Figure 4. By comparing with Figure 3, one can see that effects of collisions in the multi-level and multi-term cases have the same behaviours. However, for some cases presented in the Figure 5, the effect of collisions in the multi-term case is quantitatively different from that in the multi-level case. In particular, the levels 4 p $^2P_{3/2}$, 3 d $^2D_{3/2}$, and 4 d $^2D_{3/2}$ are more sensitive to collisions in the multi-term case compared to the case of multi-level model. On the other hand, the levels $3d\,^2D_{5/2}$ and $4d\,^2D_{5/2}$ are less sensitive to collisions in the multi-term case.

As shown above there are some differences in the sensitivity of Mg II levels to collisions with hydrogen atoms between the multi-term and multi-level cases; nevertheless, these differences are practically rather small, specially for sufficiently low n_H. For

https://doi.org/10.1017/pasa.2024.89 Published online by Cambridge University Press

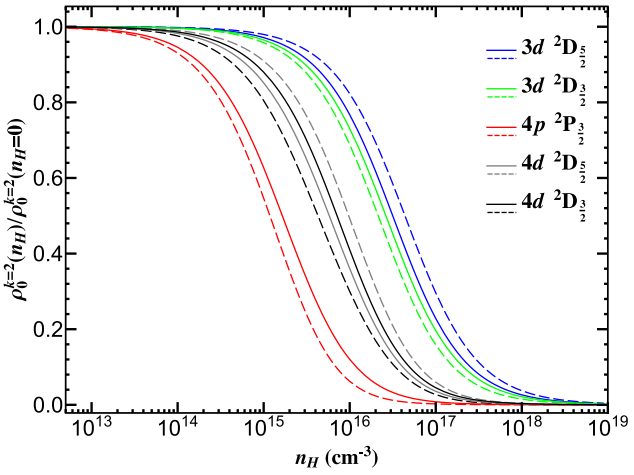

Figure 5. Comparison of the ratio $\frac{\rho_0^2(n_H)}{\rho_0^2(n_H=0)}$ as a function of n_H for the multi-term and multi-level cases. The dashed line represents the multi-term case, while the solid line represents the multi-level case.

the case of the well-known chromospheric Mg II UV h-k lines which are directly connected to the terms 3 s ^2S and 3 p ^2P, we find that collisions are not important and can be safely neglected in future studies. In fact, the term 3 s ^2S is not sensitive to collisions with hydrogen atoms because of its total angular momentum being 1/2, meaning the depolarising rates $D^{k=2}$ are zero by definition. Additionally, for the s-term there is no collisional transfer within the term since it only has one fine structure level. Moreover, the 3 p ^2P, as it is shown in Figures 3 and 4, it starts to be sensitive to collisions only for $n_H \gtrsim 10^{16}$ cm^{-3}, which is higher than the typical densities encountered in the chromosphere.

4. Conclusion

The role of the collisional processes for the Mg II lines is usually disregarded when solving the master equation for the atomic density matrix. We find that the polarization of Mg II h and k lines are not affected by collisions with neutral hydrogen. Nevertheless, we find that collisions with hydrogen atoms are important for other Mg II lines, specially those directly connected to the level 4 p $^2P_{3/2}$. Our result could help eliminate potential sources of error or uncertainty and provide clarity on the true significance of collisions for future studies. We provide all the collisional rates for the multi-level (13 levels) and multi-term (8 terms) models of Mg II in Appendix 1 of this paper.

Acknowledgements. This research work was funded by Institutional Fund Projects under grant no. (IFPIP:995-130-1443). The authors gratefully acknowledge technical and financial support provided by the Ministry of Education and King Abdulaziz University, DSR, Jeddah, Saudi Arabia

Data availability statement. Not applicable.

References

Allen, C. W., & Cox, A. N. 1999, Allen's Astrophysical quantities. New York: AIP Press.
Alsina Ballester, E., Belluzzi, L., & Trujillo Bueno, J. 2016, ApJL, 831, L15
Barklem, P. S. 1998, Ph.D. Thesis, Univ. Queensland
Barklem, P. S., & O'Mara, B. J. 1998, MNRAS, 300, 863
Belluzzi, L., & Trujillo Bueno, J. 2012, ApJL, 750, L11
Bohlin, J. D., Frost, K. J., Burr, P. T., Guha, A. K., & Withbroe, G. L. 1980, SoPh, 65, 5
Calvert, J., Griner, D., Montenegro, J., et al. 1979, OptEn, 18, 287
Cox, A. N. 2000, Allen's Astrophysical Quantities, 4th ed. (New York: Springer Verlag and AIP Press)
Derouich, M., Sahal-Bréchot, S., Barklem, P. S., & O'Mara, B. J. 2003a, A&A, 404, 763
Derouich, M., Sahal-Bréchot, S., & Barklem, P. S. 2003b, A&A, 409, 369
Derouich, M. 2004, Ph.D. Thesis, Paris VII-Denis Diderot University
Derouich, M., Sahal-Bréchot, S., & Barklem, P. S. 2004, A&A, 426, 707
Derouich, M., Sahal-Bréchot, S., & Barklem, P.S. 2005, A&A, 434, 779
Derouich, M., & Barklem, P.S. 2007 A&A, 462, 1171
Derouich, M., Trujillo Bueno, J., & Manso Sainz, R. 2007, A&A, 472, 269
Derouich, M. 2008, A&A, 481, 845
Deb, C. & Derouich, M. 2014, A&A, 572, id.A53
del Pino Alemán, T., Casini, R., & Manso Sainz, R. 2016, ApJL, 830, L24
del Pino Alemán, T., Trujillo Bueno, J., Casini, R., & Manso Sainz, R. 2020, ApJ, 891, 91
Derouich, M. 2017, NewA, 51, 32
Derouich, M., Basurah, H., Badruddin, B. 2017, PASA, 34, id.e018 8
Derouich, M. 2018, MNRAS, 481, 2444
Derouich, M. 2020, MNRAS, 491, 3990
Henze, W., & Stenflo, J. O. 1987, SoPh, 111, 243
Landi Degl'Innocenti, E., & Landolfi, M. 2004, Polarization in Spectral Lines, Vol. 307 (Dordrecht: Springer)
Leenaarts, J., Pereira, T. M. D., Carlsson, M., Uitenbroek, H., & De Pontieu, B. 2013, ApJ, 772, 89
Martin, W.C., & Wiese, W.L. 2002, Atomic, Molecular, and Optical Physics Handbook (version 1.01) [online], Available: http://physics.nist.gov/Pubs/AtSpec/index.html
Nienhuis G. 1976, J. Phys. B: Atom. Molec. Phys. 9, 167
Kurucz, R. L. 1973, SAO Special Report 351
Kurucz, R. L. 1981, SAO Special Report 390
Kurucz, R. L. 2013, kurucz.harvard.edu
Omont A. 1977, Prog. Quantum Electronics, 5, 69
Thuillier, G., Floyd, L., Woods, T. N., et al. 2004, Geophys. Monogr. 141, 171
Woodgate, B. E., Tandberg-Hanssen, E. A., Bruner, E. C., et al. 1980, SoPh, 65, 73
Sahal-Bréchot S. 1977, ApJ., 213, 887
Sahal-Bréchot, S.; Derouich, M.; Bommier, V.; Barklem, P. S. 2007, A&A, 465, 667

Appendix 1. Collisional data

Table 2. Mg II collisional rates for the multi-level case.

Term	J	J'	k	a^k	λ^k
3p ^2P	3/2	3/2	2	3.92	0.372
	1/2	3/2	0	2.94	0.493
3d ^2D	3/2	3/2	2	7.43	0.377
	5/2	5/2	2	6.62	0.383
	5/2	5/2	4	7.10	0.379
	5/2	3/2	0	6.52	0.382
	5/2	3/2	2	2.75	0.376
4p ^2P	3/2	3/2	2	23.26	0.377
	1/2	3/2	0	16.71	0.367

https://doi.org/10.1017/pasa.2024.89 Published online by Cambridge University Press

Table 2. (Continued)

Term	J	J'	k	a^k	λ^k
$4d\,^2D$	3/2	3/2	2	14.26	0.388
	5/2	5/2	2	10.75	0.382
	5/2	5/2	4	11.43	0.376
	5/2	3/2	0	10.26	0.366
	5/2	3/2	2	4.62	0.370
$4f\,^2F$	5/2	5/2	2	5.80	0.401
	5/2	5/2	4	5.55	0.373
	7/2	7/2	2	9.99	0.367
	7/2	7/2	4	4.65	0.390
	7/2	7/2	6	2.90	0.383
	5/2	7/2	0	12.02	0.376
	5/2	7/2	2	1.34	0.379
	5/2	7/2	4	0.44	0.367

Table 3. P-states: Mg II collisional rates for the multi-term case.

Term	J	J'	J''	J'''	k	a^k	λ^k
$3p\,^2P$	0.5	1.5	0.5	1.5	2	3.785	0.308
	1.5	0.5	1.5	0.5	2	3.785	0.308
	1.5	1.5	1.5	1.5	2	3.92	0.372
	0.5	0.5	1.5	1.5	0	2.94	0.493
	0.5	1.5	1.5	0.5	2	−0.045	0.210
	0.5	1.5	1.5	1.5	2	0.09	0.348
	1.5	0.5	0.5	1.5	2	−0.045	0.210
	1.5	0.5	1.5	1.5	2	−0.09	0.348
	1.5	1.5	0.5	1.5	2	0.09	0.348
	1.5	1.5	1.5	0.5	2	−0.09	0.348
$4p\,^2P$	0.5	1.5	0.5	1.5	2	15.45	0.337
	1.5	0.5	1.5	0.5	2	15.45	0.337
	1.5	1.5	1.5	1.5	2	23.26	0.377
	0.5	0.5	1.5	1.5	0	16.71	0.367
	0.5	1.5	1.5	0.5	2	−2.60	0.295
	0.5	1.5	1.5	1.5	2	5.20	0.291
	1.5	0.5	0.5	1.5	2	−2.60	0.295
	1.5	0.5	1.5	1.5	2	−5.20	0.291
	1.5	1.5	0.5	1.5	2	5.20	0.291
	1.5	1.5	1.5	0.5	2	−5.20	0.291

Table 4. $3d\,^2D$ term: Mg II collisional rates for the multi-term case.

Term	J	J'	J''	J'''	k	a^k	λ^k
$3d\,^2D$	2.5	1.5	2.5	1.5	2	8.34	0.314
	2.5	1.5	2.5	1.5	4	10.68	0.310
	1.5	2.5	1.5	2.5	2	8.34	0.314
	1.5	2.5	1.5	2.5	4	10.68	0.310
	1.5	1.5	1.5	1.5	2	7.43	0.377
	2.5	2.5	2.5	2.5	2	6.62	0.383
	2.5	2.5	2.5	2.5	4	7.10	0.379
	2.5	2.5	2.5	1.5	2	2.91	0.367
	2.5	2.5	2.5	1.5	4	1.45	0.299
	2.5	2.5	1.5	2.5	2	−2.91	0.367
	2.5	2.5	1.5	2.5	4	−1.45	0.299
	2.5	2.5	1.5	1.5	0	6.52	0.382
	2.5	2.5	1.5	1.5	2	2.75	0.376
	2.5	1.5	2.5	2.5	2	2.91	0.367
	2.5	1.5	2.5	2.5	4	1.45	0.299
	2.5	1.5	1.5	2.5	2	3.30	0.219
	2.5	1.5	1.5	2.5	4	0.513	0.255
	2.5	1.5	1.5	1.5	2	0.506	0.221
	1.5	2.5	2.5	2.5	2	−2.91	0.367
	1.5	2.5	2.5	2.5	4	−1.45	0.299
	1.5	2.5	2.5	1.5	2	3.30	0.219
	1.5	2.5	2.5	1.5	4	0.513	0.255
	1.5	2.5	1.5	1.5	2	−0.506	0.221
	1.5	1.5	2.5	1.5	2	0.506	0.221
	1.5	1.5	1.5	2.5	2	−0.506	0.221

https://doi.org/10.1017/pasa.2024.89 Published online by Cambridge University Press

Table 5. $4d\,^2D$ term: Mg II collisional rates for the multi-term case.

Term	J	J'	J''	J'''	k	a^k	λ^k
$4d\,^2D$	2.5	1.5	2.5	1.5	2	14.25	0.386
	2.5	1.5	2.5	1.5	4	6.84	0.383
	1.5	2.5	1.5	2.5	2	14.25	0.386
	1.5	2.5	1.5	2.5	4	6.84	0.383
	1.5	1.5	1.5	1.5	2	14.26	0.388
	2.5	2.5	2.5	2.5	2	10.75	0.382
	2.5	2.5	2.5	2.5	4	11.43	0.376
	2.5	2.5	2.5	1.5	2	6.04	0.356
	2.5	2.5	2.5	1.5	4	−1.85	0.329
	2.5	2.5	1.5	2.5	2	−6.04	0.356
	2.5	2.5	1.5	2.5	4	1.85	0.329
	2.5	2.5	1.5	1.5	0	10.26	0.366
	2.5	2.5	1.5	1.5	2	4.62	0.370
	2.5	1.5	2.5	2.5	2	6.04	0.356
	2.5	1.5	2.5	2.5	4	−1.85	0.329
	2.5	1.5	1.5	2.5	2	6.05	0.357
	2.5	1.5	1.5	2.5	4	−0.65	0.390
	2.5	1.5	1.5	1.5	2	0.008	0.363
	1.5	2.5	2.5	2.5	2	−6.04	0.356
	1.5	2.5	2.5	2.5	4	1.85	0.329
	1.5	2.5	2.5	1.5	2	6.05	0.357
	1.5	2.5	2.5	1.5	4	−0.65	0.390
	1.5	2.5	1.5	1.5	2	−0.008	0.363
	1.5	1.5	2.5	1.5	2	0.008	0.363
	1.5	1.5	1.5	2.5	2	−0.008	0.363

Table 6. $4f\,^2F$ term: Mg II collisional rates for the multi-term case.

Term	J	J'	J''	J'''	k	a^k	λ^k
$4f\,^2F$	3.5	2.5	3.5	2.5	2	9.36	0.331
	3.5	2.5	3.5	2.5	4	7.22	0.358
	3.5	2.5	3.5	2.5	6	−3.68	0.398
	2.5	3.5	2.5	3.5	2	9.36	0.331
	2.5	3.5	2.5	3.5	4	7.22	0.358
	2.5	3.5	2.5	3.5	6	−3.68	0.398
	2.5	2.5	2.5	2.5	2	5.80	0.401
	2.5	2.5	2.5	2.5	4	5.55	0.373
	3.5	3.5	3.5	3.5	2	9.99	0.367
	3.5	3.5	3.5	3.5	4	4.65	0.390
	3.5	3.5	3.5	3.5	6	2.90	0.383
	3.5	3.5	3.5	2.5	2	−2.17	0.423
	3.5	3.5	3.5	2.5	4	2.10	0.435
	3.5	3.5	3.5	2.5	6	−12.51	0.382
	3.5	3.5	2.5	3.5	2	2.17	0.423
	3.5	3.5	2.5	3.5	4	−2.10	0.435
	3.5	3.5	2.5	3.5	6	12.51	0.382
	2.5	2.5	3.5	3.5	0	12.02	0.376
	2.5	2.5	3.5	3.5	2	1.34	0.379
	2.5	2.5	3.5	3.5	4	0.44	0.367
	3.5	2.5	3.5	3.5	2	−2.17	0.423
	3.5	2.5	3.5	3.5	4	2.10	0.435
	3.5	2.5	3.5	3.5	6	−12.51	0.382
	3.5	2.5	2.5	3.5	2	0.234	0.469
	3.5	2.5	2.5	3.5	4	0.889	0.298
	3.5	2.5	2.5	3.5	6	−3.61	0.368
	3.5	2.5	2.5	2.5	2	2.75	0.388
	3.5	2.5	2.5	2.5	4	−0.997	0.266
	2.5	3.5	3.5	3.5	2	2.17	0.423
	2.5	3.5	3.5	3.5	4	−2.10	0.435
	2.5	3.5	3.5	3.5	6	12.51	0.382
	2.5	3.5	3.5	2.5	2	0.234	0.469
	2.5	3.5	3.5	2.5	4	0.889	0.298
	2.5	3.5	3.5	2.5	6	−3.61	0.368
	2.5	3.5	2.5	2.5	2	−2.75	0.388
	2.5	3.5	2.5	2.5	4	0.997	0.266
	2.5	2.5	3.5	2.5	2	2.75	0.388
	2.5	2.5	3.5	2.5	4	−0.997	0.266
	2.5	2.5	2.5	3.5	2	−2.75	0.388
	2.5	2.5	2.5	3.5	4	0.997	0.266

https://doi.org/10.1017/pasa.2024.89 Published online by Cambridge University Press